Check for updates

Small pyramidal textured ultrathin crystalline silicon solar cells with double-layer passivation

XINYU TAN,[1] WENSHENG YAN,[2,3,*] YITENG TU,[2] AND CAN DENG[1]

[1]*College of Materials and Chemical Engineering, Key laboratory of inorganic nonmetallic crystalline and energy conversion materials (CTGU), China Three Gorges University, 8 University Avenue, Yichang 443002, China*
[2]*College of Electrical Engineering & New Energy, Hubei Provincial Collaborative Innovation Center for New Energy Microgrid, China Three Gorges University, 8 University Avenue, Yichang 443002, China*
[3]*Karlsruhe Institute of Technology, Institute of Microstructure Technology, Hermann-von-Helmholtz-Platz 1, 76344 Eggenstein-Leopoldshafen, Germany*
[*]*yws118@gmail.com*

Abstract: Ultrathin crystalline silicon solar cells are a promising technology roadmap to achieve more cost effectiveness. However, experimental reports on ultrathin crystalline silicon cells with thickness less than 20 μm are rare. Here, we experimentally fabricate and investigate ultrathin monocrystalline silicon solar cells consisting of 16 μm-silicon base thickness and low-cost front random pyramidal texture with the feature size of 1-2 μm. The normalized light absorption is calculated to explain the measured external quantum efficiency. The achieved efficiency is 15.1% for the single-layer passivated textured solar cell. In addition, via double-layer passivation of Al_2O_3/SiN_x, the efficiency is further increased to 16.4% for the best textured cell, which significantly improves the absolute efficiency with $\Delta\eta = 1.3\%$.

OCIS codes: (040.5350) Photovoltaic; (040.6040) Silicon; (250.0250) Optoelectronics.

References and links

1. See www.itrpv.net for the international technology roadmap for photovoltaic results (2015).
2. K. X. Wang, Z. Yu, V. Liu, Y. Cui, and S. Fan, "Absorption enhancement in ultrathin crystalline silicon solar cells with antireflection and light-trapping nanocone gratings," Nano Lett. **12**(3), 1616–1619 (2012).
3. W. Zhu, F. Xiao, I. D. Rukhlenko, J. Geng, X. Liang, M. Premaratne, and R. Jin, "Wideband visible-light absorption in an ultrathin silicon nanostructure," Opt. Express **25**(5), 5781–5786 (2017).
4. I. Kim, D. S. Jeong, W. S. Lee, W. M. Kim, T. S. Lee, D. K. Lee, J. H. Song, J. K. Kim, and K. S. Lee, "Silicon nanodisk array design for effective light trapping in ultrathin c-Si," Opt. Express **22**(S6 Suppl 6), A1431–A1439 (2014).
5. Y. Huang, W. Wang, W. Pan, W. Chen, Z. Wang, X. Tan, and W. Yan, "Comparative investigation on designs of light absorption enhancement of ultrathin crystalline silicon for photovoltaic applications," J. Photonics Energy **6**(4), 047001 (2016).
6. A. Bozzola, P. Kowalczewski, and L. C. Andreani, "Towards high efficiency thin-film crystalline silicon solar cells: The roles of light trapping and non-radiative recombinations," J. Appl. Phys. **115**(9), 094501 (2014).
7. A. Mavrokefalos, S. E. Han, S. Yerci, M. S. Branham, and G. Chen, "Efficient light trapping in inverted nanopyramid thin crystalline silicon membranes for solar cell applications," Nano Lett. **12**(6), 2792–2796 (2012).
8. W. Yan, S. Dottermusch, C. Reitz, and B. S. Richards, "Hexagonal arrays of round-head silicon nanopillars for surface anti-reflection applications," Appl. Phys. Lett. **109**(14), 143901 (2016).
9. R. A. Pala, S. Butun, K. Aydin, and H. A. Atwater, "Omnidirectional and broadband absorption enhancement from trapezoidal Mie resonators in semiconductor metasurfaces," Sci. Rep. **6**(1), 31451 (2016).
10. C. Trompoukis, I. Massiot, V. Depauw, O. El Daif, K. Lee, A. Dmitriev, I. Gordon, R. Mertens, and J. Poortmans, "Disordered nanostructures by hole-mask colloidal lithography for advanced light trapping in silicon solar cells," Opt. Express **24**(2), A191–A201 (2016).
11. C. Trompoukis, O. E. Daif, V. Depauw, I. Gordon, and J. Poortmans, "Photonic assisted light trapping integrated in ultrathin crystalline silicon solar cells by nanoimprint lithography," Appl. Phys. Lett. **101**(10), 103901 (2012).

12. M. S. Branham, W. C. Hsu, S. Yerci, J. Loomis, S. V. Boriskina, B. R. Hoard, S. E. Han, and G. Chen, "15.7% Efficient 10-μm-thick crystalline silicon solar cells using periodic nanostructures," Adv. Mater. **27**(13), 2182–2188 (2015).
13. S. Jeong, M. D. McGehee, and Y. Cui, "All-back-contact ultra-thin silicon nanocone solar cells with 13.7% power conversion efficiency," Nat. Commun. **4**, 2950 (2013).
14. L. Wang, A. Lochtefeld, J. Han, A. P. Gerger, M. Carroll, J. Ji, A. Lennon, H. Li, R. Opila, and A. Barnett, "Development of a 16.8% Efficient 18-μm SiliconSolar Cell on Steel," IEEE J. Photovoltaics **4**(6), 1397–1404 (2014).
15. W. Yan, Z. Tao, M. Gu, and B. S. Richards, "Photocurrent enhancement of ultrathin front-textured crystalline silicon solar cells by rear-located periodic silver nanoarrays," Sol. Energy **150**, 156–160 (2017).
16. H. Savin, P. Repo, G. von Gastrow, P. Ortega, E. Calle, M. Garín, and R. Alcubilla, "Black silicon solar cells with interdigitated back-contacts achieve 22.1% efficiency," Nat. Nanotechnol. **10**(7), 624–628 (2015).
17. E. D. Palik, *Handbook of Optical Constants of Solids* (Elsevier, 1998).
18. M. A. Green, "Self-consistent optical parameters of intrinsic silicon at 300 K including temperature coefficient," Sol. Energy Mater. Sol. Cells **92**(11), 1305–1310 (2008).

1. Introduction

Crystalline silicon (c-Si) solar cells are the most important part of photovoltaics (PV) family. Over the past tens of years, c-Si solar cells have dominated the global PV market with the share of more than 90% [1]. On the other hand, however, c-Si material alone occupies up to 40% of the module cost and thus it is promising to achieve more cost-effectiveness via the technology roadmap of ultrathin c-Si solar cells.

Up to now, there are already a great number of reports about optical design and fabrication in the area of ultrathin c-Si solar cells [2–10]. However, experimental investigations on the device fabrication and the efficiency of ultrathin c-Si solar cells with thickness less than 20 μm are rare [11–15]. This is mainly due to that compared with simulation and optical structural fabrication, it is much more challenging to prepare ultrathin c-Si solar cells, let alone good cell efficiency achieved.

In this work, we experimentally investigate ultrathin monocrystalline c-Si solar cells consisting of 16 μm-silicon base thickness. Our ultrathin monocrystalline silicon solar cells are single-sided front textured, which is based on two reasons: (i) At present, most experimental reports on ultrathin c-Si solar cells are single-sided front textured, which is relevant to the current state of the art; (ii) our c-Si is on a steel substrate and thus only front-sided texture is conducted for the present case. For the front texture, one could choose either nano-scale texture or micron-scale texture. Both of the two options have pros and cons. For example, for nano-scale surface texture in the form of various geometries, the benefit could be higher photocurrent because of higher light trapping compared with micron-scale texture. However, some of nanofabrication methods are expensive like electron beam lithography (EBL), which is actually not suitable for large-scale application. Some of nanofabrication methods are not mature for PV industry applications at present. For micro-scale pyramidal texture via NaOH or KOH solution, the photocurrent is slightly lower than nano-scale texture in terms of the light absorption enhancement. But, the wet-etching preparation of pyramidal texture is not only very cheap but also mature for large-scale PV industrial application. In the present work, we chose pyramidal surface texture via the wet-etching method and the motivation is towards the PV industry application. In this work, the pyramidal feature size is in the range of 1-2 μm rather than conventional 3-10 μm. Compared with industrial standard pyramidal texture in the range of 3-10 μm, the small pyramidal texture in the range of 1-2 μm can more effectively increase the total path of light propagation in silicon and thereby improve photocurrent. For thin crystalline silicon less than 20 μm, it is difficult to prepare the pyramidal texture with the range of 3-10 μm ensuring high yield of solar cells. In contrast, small pyramidal texture in the range of 1-2 μm is beneficial to ultrathin c-Si solar cell preparations.

Double-layer passivation offers a unique opportunity to significantly increase the efficiency. The positive role of double-layer passivation of Al_2O_3/SiN_x has been investigated in thick c-Si solar cells [16]. However, the reports on the applications of double-layer

passivation to ultrathin c-Si solar cells with thickness less than 20 µm are rare. Therefore, it is necessary and significant to investigate the effect of double-layer passivation on the ultrathin c-Si solar cells. As a result, we not only fabricate ultrathin c-Si solar cells but also investigate the effect of double-layer passivation of Al_2O_3/SiN_x on photovoltaic performance. To explain the measured external quantum efficiency (EQE), we calculate the normalized light absorption as a function of wavelength in the range of 300 to 1100 nm. The achieved efficiency is 15.1% for the single-layer passivated front textured silicon solar cell. The best efficiency of 16.4% is achieved for the textured ultrathin c-Si solar cells via front double-layer passivation, which significantly improves the absolute efficiency with $\Delta\eta = 1.3\%$.

2. Solar cell fabrication and characterizations

2.1 Fabrication of solar cells

The present work adopts the architecture of solar cells with passivated emitter and rear cell (PERC). Here, p-type silicon on the steel substrate is used and the cell consists of typical p-n diffusion junction. A small-sized pyramidal surface texture with feature size of 1-2 µm is conducted by home-made wet-etching procedure. Figures 1(a)-1(d) shows a scanning electron microscope (SEM) image of pyramidal texture surface Fig. 1(a), cross-sectional schematic of the front textured ultrathin solar cell Fig. 1(b), photo of the solar cell device Fig. 1(c), and cross-sectional SEM image of the device Fig. 1(d), respectively. For single-layer passivation, 80 nm thick SiN_x is deposited by plasma enhanced chemical vapour deposition. For double-layer passivation of Al_2O_3/SiN_x, ultrathin Al_2O_3 layer of 3 nm is prepared via atomic layer deposition and SiN_x thickness is 80 nm, where Al_2O_3 layer is deposited prior to SiN_x thin film.
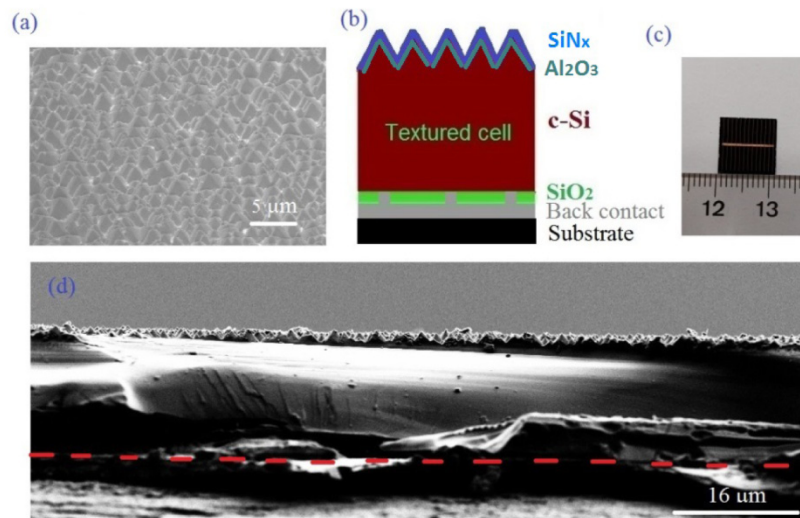

Fig. 1. SEM view of front pyramidal texture (a); Schematic of the ultrathin c-Si solar device (b); Photo of the device (c); and Cross-sectional SEM image of the solar cell (d). The red dashed line indicates the boundary between silicon and the substrates.

2.2 Characterizations of solar cells

Structural characterizations and photovoltaic performance are conducted. SEM measurements are conducted to obtain the morphologies of front texture and cross-sectional solar device, respectively. The EQE of solar cells is characterized by using the QEX10 Solar Cell Quantum Efficiency/IPCE/Spectral Response Measurement System. The photovoltaic responses of the solar cells with the area of approximately 1 cm^2, as shown in Fig. 1(c), are measured under

standard test conditions (air-mass 1.5 illumination with a light intensity of 100 mW/cm^2 at a temperature of 25°C). As a result, the three photovoltaic parameters (namely, short-circuit current density J_{sc}, open-circuit voltage V_{oc}, and fill factor FF) are measured and thus the cell efficiency (η) are obtained.

3. Results and discussion

Figure 2 shows the measured EQE as a function of wavelength in the range of 300 to 1100 nm, where single-layer passivated planar and front textured ultrathin c-Si solar cells are shown for the completeness. It is seen in Fig. 2 that the present ultrathin c-Si solar cells show excellent EQE responses in the wavelength range of 300 to 1100 nm. In addition, it is found that the EQE response of the textured ultrathin c-Si solar cell shows a significant enhancement in a broadband range compared with the planar cell. This is obviously due to front small-sized pyramidal texture, which remarkably increases the total propagation length or light absorption in silicon. According to the measured photocurrent, the small-sized pyramidal texture leads to the enhancement of 38.7% compared with the planar cell.

To explain the difference of EQEs between the planar and textured c-Si cells, we calculate the wavelength-dependent normalized light absorption for the two solar cells. Here, the finite-difference time-domain (FDTD) method is adopted. In the present simulation, the Lumerical's FDTD software is used. To calculate the wavelength dependent absorption, we adopted an SEM of the present small pyramidal texture in our simulation, where the small mesh size of 1 nm is set. A normally incident plane wave with a wavelength range from 300 to 1100 nm is used for the simulation source. Complex optical constants (n, k) are required to implement the present simulations, where the complex constants of SiO$_2$, c-Si, and SiN$_x$ are from the literatures [4, 17, 18]. The calculated results are shown in Fig. 3. It is seen in Fig. 3 that compared with the planar cell, the calculated light absorption of the textured silicon cell shows a significant enhancement in the whole wavelength range of 300 to 1100 nm. The calculated results are consistent in trend with the measured EQE results. It is normal that the calculated light absorption is much higher than the measured EQE, which is due to the fact that the former only includes the light absorption. As shown in Fig. 3, the absorption simulation of the planar cell shows small absorption oscillation in the longer wavelengths, which is relevant to the thickness of silicon. Previous simulation showed that the phenomenon of absorption oscillation is more obvious in thinner planar silicon [5].
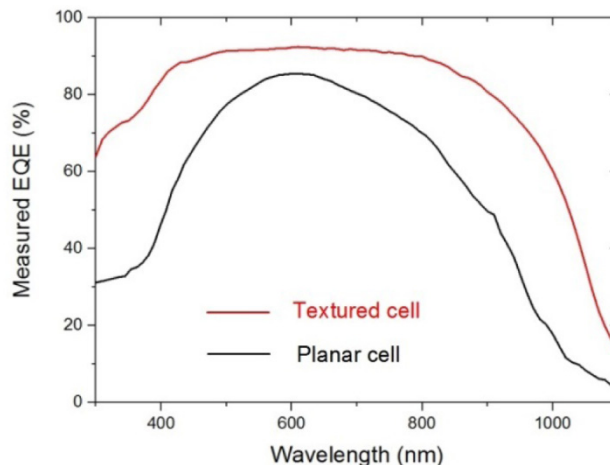

Fig. 2. Measured EQE curves of the planar and textured silicon cells in the wavelength range of 300 to 1100 nm.
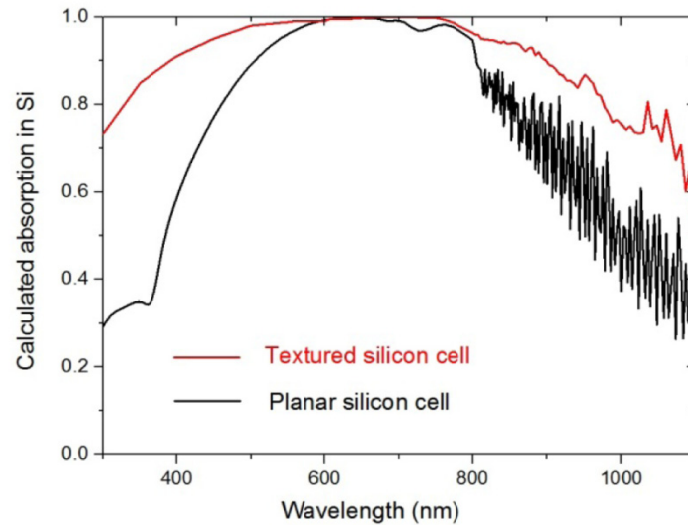
Fig. 3. Calculated wavelength dependent light absorption of the planar and textured silicon cells in the wavelength range of 300 to 1100 nm.

It is interesting to compare the light absorption distribution between the planar and textured silicon solar cells as it is expected to be very different. Here, we made an approximation treatment on simulation, where each of pyramids has the height of 2 µm and base width of 2 µm, and silicon base thickness of 16 µm. For the planar silicon cell, silicon thickness of 18 µm is used. This treatment is close to the real case. In addition, it is time-saving in simulation because only one periodic structure needs to be calculated. The calculated results of light absorption distribution of the planar and textured silicon cells are shown in Fig. 4, where three wavelengths of 400 nm, 700 nm, and 1000 nm are given as example demonstration. Note that the scale bars of the absorption density are different in Figs. 4(a)-4(f). It can be seen in Fig. 4 that light absorption density distributions are obviously different between the planar and textured silicon cells. In addition, for the planar cell, the absorption density intensity is constant along x axis at arbitrary z value. In contrast, the absorption density intensity is variable along x axis at arbitrary z value for the textured cell.
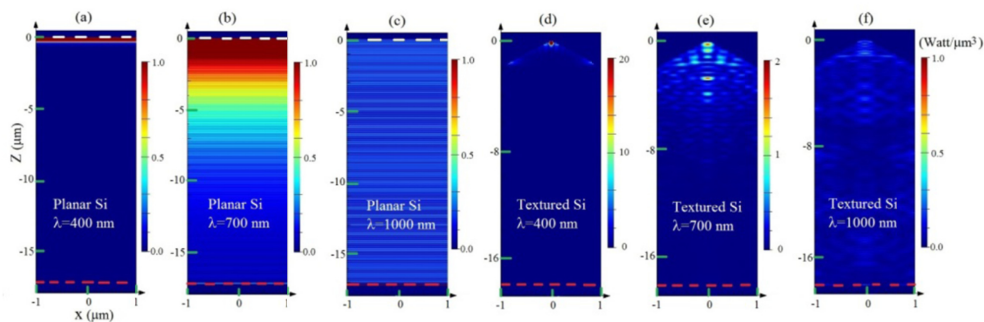

Fig. 4. Two-dimensional light absorption density distribution profiles for the planar and textured silicon cells at the three wavelengths. The calculation results are shown for the planar silicon cell at 400 nm (a), 700nm (b), and 1000 nm (c) and for the textured silicon cell at 400 nm (d), 700nm (e), and 1000 nm (f), respectively. The white dashed lines indicate the boundary between silicon and air whereas the red dashed lines define the boundary between silicon and the substrate.

The measured *J-V* responses of the textured solar cells with single-layer and double-layer passivation are shown in Fig. 5, respectively. It is found that compared with the single-layer passivated solar cell, the double-layer passivated cell shows an improved response curve with higher photocurrent and open-circuit voltage. To present more details, the measured photovoltaic parameters including J_{sc}, V_{oc}, *FF*, and η are listed in Table 1, where the three solar cells are given. It is found in Table 1 that the J_{sc} value and the efficiency are 23.5 mA/cm^2 and 10.6% for the planar c-Si solar cell with single-layer passivation, respectively. When the front texture is applied, J_{sc} is enhanced to 32.6 mA/cm^2, which is due to the increased light absorption via the surface texture. The efficiency is significantly improved to 15.1%. Furthermore, when front double-layer passivation of Al_2O_3/SiN_x is applied, it is found that the J_{sc} value is further improved to 34.0 mA/cm^2. At the same time, the V_{oc} experiences an obvious increase with ΔV_{oc} = 29 mV. As a result, the efficiency of 16.4% is obtained for the double-layer passivated textured cell. Compared with single-layer passivated textured c-Si cell, the absolute efficiency of $\Delta \eta$ = 1.3% is achieved for the textured c-Si cell with double-layer passivation.

Totally, we have measured ten ultrathin silicon solar cells with double-layer passivation. It is found that the efficiency improvement is in the range of 0.9% to 1.3% for these solar cells compared with the cells with single-layer passivation. The best cell shows the efficiency enhancement of 1.3%. For the planar cells, the efficiency improvement via double-layer passivation is slightly better than the textured silicon solar cells, which should be due to better surface quality. In the majority of previous experimental reports about ultrathin crystalline silicon solar cells, it either adopted nanostructured silicon surface or single-layer surface passivation. Compared with nanotextured silicon surface via the EBL fabrication [12], the present wet-etching method for small pyramidal texture is very cheap and easily up-scalable. In addition, the wet-etching texturing method has adapted to the industrial application. On the other hand, at present, the reported efficiencies have still big room to the theoretical limit. Therefore, a variety of approaches should be conducted to make the efficiency progress. Compared with single-layer passivation, this work demonstrates that double-layer passivation can significantly improve the efficiency of ultrathin silicon solar cells.
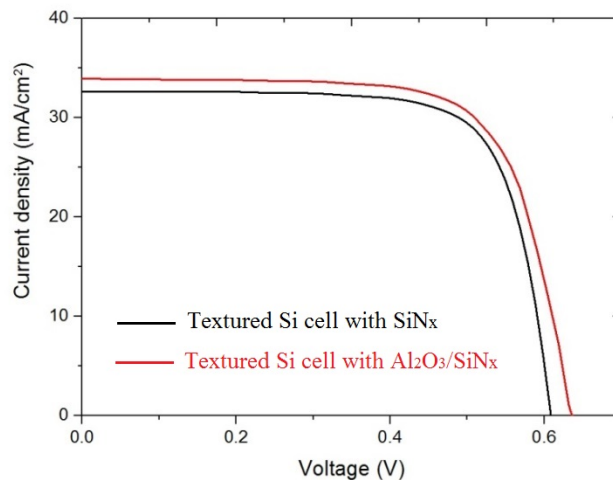

Fig. 5. J-V responses of the textured ultrathin c-Si cells with SiN_x passivation and Al_2O_3/SiN_x passivation, respectively.

Table 1. Photovoltaic parameters of the planar ultrathin c-Si cell and the textured ultrathin c-Si with single-layer passivation of SiN$_x$ and double-layer passivation of Al$_2$O$_3$/SiN$_x$.

Devices	$J_{sc}(mA/cm^2)$	$V_{oc}(\mathrm{mV})$	$FF(\%)$	$\eta(\%)$
Planar cell (SiN$_x$)	23.5	611	0.740	10.6%
Texture cell (SiN$_x$)	32.6	608	0.764	15.1%
Texture cell (Al$_2$O$_3$/SiN$_x$)	34.0	637	0.759	16.4%

4. Conclusion

In summary, ultrathin c-Si solar cells are a promising pathway to achieve more cost-effectiveness. Up to now, but, the experimental investigations about the fabrication and efficiency of ultrathin c-Si solar cells with thickness less than 20 µm are few due to more challenges compared with simulation and optical structural fabrication. In addition, the investigations on the effect of double-layer passivation on PV performance are also rare for the ultrathin c-Si solar cells less than 20 µm. In this work, we not only fabricate ultrathin monocrystalline silicon solar cells but also investigate the effect of double-layer passivation on the photovoltaic performance. The excellent efficiency of 15.1% is achieved for the single-layer passivated textured c-Si solar cells. Double-layer passivation increases the efficiency with the result of 16.4%, which is benefited from improvements in both the short-circuit current density and the open-circuit voltage. As a result, the absolute efficiency increase of $\Delta\eta$ = 1.3% is obtained. It is expected that this work is useful to develop the ultrathin c-Si solar cells towards higher efficiency and industrial applications.